

# USING THE ANALYTICAL CALCULATION METHOD FOR COOLING SYSTEMS STUDYING

*R.P. Slabospitsky, M.A. Khazhmuradov\*, V.P. Lukyanova, S.I. Prokhorets*

*National Science Center "Kharkov Institute of Physics and Technology", 61108, Kharkov, Ukraine*

(Received January 22, 2013)

An analytical method for calculating the air flow battery cooling with non-uniform heat distribution in the battery cells is considered. The calculations were done for different air rates and directions. It is shown that to ensure the normal battery operation the air flow rates must be greater than 2 m/s.

PACS: 44.15.+a

## 1. INTRODUCTION

Among the wide variety of cooling systems used in computer, consumer and military devices, much attention is paid to the accumulator battery cooling systems. For battery normal operation its temperature must be within  $-30^{\circ}\text{C} \dots +50^{\circ}\text{C}$ . Such temperature regime must be ensured with battery cooling system, which in turn should be compact, light, affordable and able to work in different environments. Structurally, battery consists from the individual cells, the number of which may be large. The case of battery air cooling is considered in this article.

During the parallel cooling the air flow can be supplied from the bottom, top or side of the battery, pass through the channels between the battery cells and go out into the environment.

Cooling system functioning can be analyzed either by analytical calculations or by numerical simulation. We use the analytical calculations to describe the processes in the battery cooling system [1-6]. The article specifies and summarizes the results presented earlier in [7-9], where battery cooling system was analyzed and simulated for air supplied from the bottom of the battery [7], from the top of battery with varying cell gap [8] and from the battery lateral surface [9]. Previous results are complemented by more detailed analysis, from which more complete conclusions followed - how to achieve stable battery operation in the permissible temperature range  $-30^{\circ}\text{C} \dots +50^{\circ}\text{C}$ .

## 2. ANALYTICAL CALCULATION METHOD

Calculations are considered for the specific battery cooling system. The scheme of the entire battery is shown at Fig.1, which also shows the battery cell sizes, the cooling air flow is supplied through the rectangular channel.

Such channel is now widely used in batteries, since the cells are made from the rectangular plates.

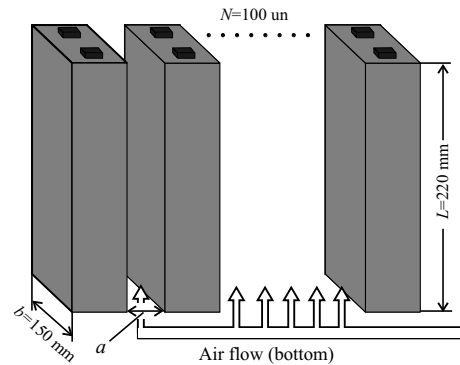


*Fig.1. Battery scheme with air cooling through the rectangular channel ( $a = 2, 3, 4, 5 \text{ mm}$ )*

Cooling of the battery cell surfaces with air flow passing through the channels is defined by the equations of energy and momentum conservation [1]

$$\begin{aligned} u \frac{\partial u}{\partial x} + \nu \frac{\partial u}{\partial y} &= v \left( \frac{\partial^2 u}{\partial y^2} \right), \\ u \frac{\partial T}{\partial x} + \nu \frac{\partial T}{\partial y} &= \alpha \left( \frac{\partial^2 T}{\partial y^2} \right), \end{aligned} \quad (1)$$

where:  $u$  - local air rate along the surface;  $\nu$  - specific volume;  $v = \mu/\rho$  - kinematic viscosity coefficient;  $T$  - temperature;  $\mu$  - dynamic viscosity coefficient;  $\alpha$  - thermal diffusivity.

These equations take into account the Prandtl number ( $Pr$ ), which is defined as follows

$$Pr = v/\alpha = (\mu/\rho)/(k/\rho \cdot C_p), \quad (2)$$

where:  $\mu$  - dynamic viscosity coefficient;  $\rho$  - density;  $k$  - thermal diffusivity;  $C_p$  - specific heat capacity at the constant pressure.

Solving the system of equations (1) can be the

\*Corresponding author E-mail address: khazhm@kipt.kharkov.ua

basic equation of energy balance

$$q_c = h_c \cdot A \left( T_s - \frac{T_{b1} + T_{b2}}{2} \right) = \dot{m} \cdot C_p (T_{b2} - T_{b1}), \quad (3)$$

where:  $q_c$  - heat flux entering the channel;  $h_c$  - heat-transfer coefficient;  $A$  - total area of the air contact with heat-transfer surface;  $\dot{m}$  - air-mass flow;  $C_p$  - specific heat capacity;  $T_{b1}$  - flow temperature at the channel input;  $T_{b2}$  - flow temperature at the channel output;  $T_s$  - average wall temperature. In equation (3) term  $(T_{b1} + T_{b2})/2$  takes into account mass-average air temperature.

Let's denote  $\Delta T_1$  - flow temperature difference at the channel input and output  $\Delta T_1 = T_{b2} - T_{b1}$ ,  $\Delta T_2$  - temperature difference between cell surface  $T_s$  and average flow temperature  $\Delta T_2 = T_s - (T_{b1} + T_{b2})/2$ . Then the equation (3) transforms into

$$q_c = h_c \cdot A \cdot \Delta T_2 = \dot{m} \cdot C_p \cdot \Delta T_1. \quad (4)$$

From the equation (4) follows that temperature difference between cell surface  $T_s$  and average flow temperature

$$\Delta T_2 = \frac{q_c}{h_c \cdot A}, \quad (5)$$

and flow temperature difference at the channel input and output

$$\Delta T_1 = \frac{q_c}{\dot{m} \cdot C_p}. \quad (6)$$

As heat is released from the cell through the entire cell surface, the area of contact with the heat transfer surface is defined as

$$A = 2b \cdot L, \quad (7)$$

where  $b$  and  $L$  - battery cell sizes (Fig. 1).

Air-mass flow through the channel equals

$$\dot{m} = \rho \cdot B \cdot V_m, \quad (8)$$

where  $\rho$  - air density,  $B$  - channel area ( $B = a \cdot b$ ),  $V_m$  - air flow rate.

Air motion in the channel can be laminar or turbulent (air resistance in the channel is much lower for laminar flow than for turbulent). Motion type is determined by the Reynolds number ( $Re$ ), and the transition boundary between laminar and turbulent motion is defined [2] by critical Reynolds number  $Re_{cr} \approx 2000$  ( $Re < 2000$  - laminar,  $Re > 2000$  - turbulent flow)

$$Re = \frac{V_m \cdot D_h}{\nu}, \quad (9)$$

where  $V_m$  - average air rate,  $\nu$  - kinematic viscosity coefficient,  $D_h$  - hydraulic diameter

$$D_h = 4 \frac{\text{square of the air flow cross-section}}{\text{wettable perimeter}}. \quad (10)$$

For rectangular channel [2]

$$D_h = 2 \left( \frac{a \cdot b}{a + b} \right), \quad (11)$$

where  $a$  - channel width,  $b$  - channel height. For considered channel (for  $a \ll b$ )  $D_h = 2a$ .

To calculate  $\Delta T_2$  and  $T_s$  values it is necessary to know  $h_c$  value - heat-transfer coefficient, which is calculated by the formula

$$h_c = \frac{k \cdot Nu}{D_h}, \quad (12)$$

where  $Nu$  - Nusselt number,  $k$  - air heat conductivity.

Nusselt number is calculated according to different formulas depending on the air flow type in the channels (laminar or turbulent flow). For laminar flow  $Nu_{lam}$  is calculated as

$$Nu_{lam} = 1.86 (Re \cdot Pr)^{0.33} \frac{D_h}{L}^{0.33} \frac{\mu_b}{\mu_s}^{0.14}, \quad (13)$$

where:  $Re$  - Reynolds number;  $Pr$  - Prandtl number;  $D_h$  - hydraulic diameter;  $L$  - channel length;  $\mu_b$ ,  $\mu_s$  - air dynamic viscosity coefficients for temperature  $+20^\circ\text{C}$  and  $+50^\circ\text{C}$  respectively.

For turbulent flow  $Nu_{turb}$  is calculated as

$$Nu_{turb} = 0.023 Re^{0.8} \cdot Pr^{0.3}, \quad (14)$$

where  $Re$  - Reynolds number,  $Pr$  - Prandtl number.

Due to the friction at the channel walls air pressure  $\Delta p$  along the channel length [3] falls by

$$\Delta p = 2f \cdot \rho \cdot V_m^2 \cdot \frac{L}{D_h}, \quad (15)$$

where  $f = 24 \cdot Re^{-1}$ ,  $\rho$  - air density,  $V_m$  - air rate,  $L$  - channel length,  $D_h$  - hydraulic diameter.

Reference and design data that we used for the calculation of the battery cooling system are shown in Table 1.

### 3. THE CALCULATION OF THE BATTERY COOLING SYSTEM FOR AIR SUPPLY FROM BELOW

Battery cooling system, shown at Fig. 1, should provide battery temperature within  $-30^\circ\text{C} \dots +50^\circ\text{C}$ , i.e. normal operating conditions the battery. If we suppose that the temperature of the battery cell surfaces  $T_s$  is almost equal to the temperature inside the battery, it is necessary to calculate  $T_s$  value dependence on various parameters such as:  $V_m$  - air flow rate;  $a$  - the gap between battery cells;  $T_{b1}$  - air temperature at the channel input;  $b$  and  $L$  sizes of battery cells and others.

These calculations were done using formula from Section 2. While determining the average temperature of the battery walls  $T_s$  we calculated Reynolds number -  $Re$ , Nusselt number -  $Nu$ , the heat transfer coefficient -  $h_c$ , the air temperature difference at the channel input and output -  $\Delta T_1$ , the temperature difference of temperature between the cell surface and the average air flow temperature -  $\Delta T_2$ .

Reynolds number determines the motion type of movement (laminar or turbulent).

Nusselt number for laminar flow  $Nu_{lam}$  is calculated by the formula (13), and for the turbulent  $Nu_{turb}$  by (14). Calculations of other parameters don't depend on the motion type.

**Table 1.** Reference and design data for the calculation of the battery cooling system

Power, released in battery cell (heat flow)	$q_c=15$ W
Battery cell width	$b=150$ mm
Battery cell height	$L=200$ mm
Gap between battery cells (channel width)	$a=2, 3, 4, 5$ mm
Air flow rate in the channel	$V_m=1..20$ m/s
Air temperature at the channel input	$T_{b1}=20^\circ\text{C}$
Air density	$\rho \approx 1.1\text{kg/m}^3$
Air heat conductivity	$k=0.0265$ W/m $\cdot^\circ\text{C}$
Air kinematic viscosity coefficient	$\nu=17.6 \cdot 10^{-6}$ m $^2$ /s
Air dynamic viscosity coefficient for temperature +20°C	$\mu_b=18.2 \cdot 10^{-6}$
Air dynamic viscosity coefficient for temperature +50°C	$\mu_s=19.5 \cdot 10^{-6}$
Prandtl number for air	$Pr=0.71$
Specific heat capacity at constant pressure	$C_p=1014$ J/kg $\cdot$ degree

In [7-9], we calculated the cooling system with heat uniform distribution in the cell. However, the really working battery is not this case. As it can be seen from Fig.2 [4], in the top of the cell temperature is higher than at the bottom.

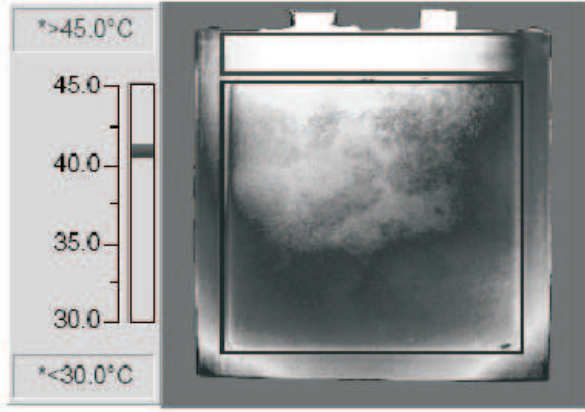


**Fig.2.** Temperature distribution in the battery cell

In this paper we'll consider only the cooling system with a non-uniform heat distribution in the cell.

Considering the cooling system when the air supply from below, we'll divide the cell wall into four equal parts each 0.055 m high. Let's say that from the 15 watts for the entire battery at the lowest (first) part of the cell 2 W is released, at the second in height - 3 W, at the third - 4 W and at the top - 6 W. The cooling air is supplied from below (Fig. 3).

**The calculation for the laminar flow.** At the first stage we made calculations for air rate of 1m/s, and the gap between the cells of 2 mm.

In this case, the Reynolds number is calculated by the formula (9) and equals to  $Re=227$ , i.e. airflow is laminar.

Nusselt number according to (13) equals to  $Nu=2.6$ .

After Nusselt number calculation heat transfer coefficient is obtained from formula (12) and equals to  $h_c=17.4$  W/m $^2$  $\cdot$ degree. If we know the heat transfer coefficient we can cal-

culate the temperature difference of temperature between the cell surface and the average air flow temperature -  $\Delta T_2$  using the formula (5).

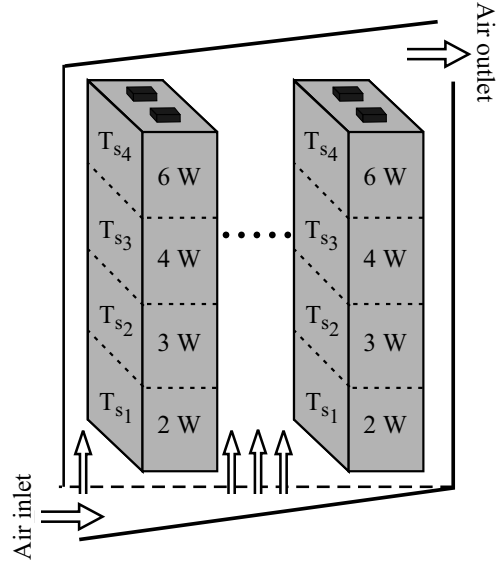


**Fig.3.** Released power distribution in the battery cell with air supplied from below:  $T_{s1}, T_{s2}, T_{s3}, T_{s4}$  - surface temperatures for the first (lowest), second, third, fourth (upper) parts respectively

Then for the first (lowest) cell part we calculated value  $\Delta T_{21} = q_c / (h_c \cdot A) = 6.9^\circ\text{C}$  ( $q_c=2$  W,  $h_c = 17.4$  W/m $^2$  $\cdot$ degree,  $A = 2 \cdot 0.055 \text{ m} \cdot 0.15 \text{ m}$ ). Using formula (8) we calculated air-mass flow for the channel with area  $B = a \cdot b = 300$  mm $^2$  ( $\dot{m} = 0.328$  g/s  $\approx 0.33$  l/s through one channel and 33l/s through 100 battery channels). Knowing  $\dot{m}$  gives us from formula (6)  $\Delta T_1$  value - flow temperature difference at the channel input and output for the first cell part,  $\Delta T_{11} = 5.9^\circ\text{C}$ . For the second cell part  $\Delta T_{22} = 10.4^\circ\text{C}$ , and temperature increases by  $\Delta T_{12} = 8.9^\circ\text{C}$ . For the third cell part  $\Delta T_{23} = 14^\circ\text{C}$ , and temperature increases by  $\Delta T_{13} = 11.9^\circ\text{C}$ . For the fourth cell part  $\Delta T_{24} = 20.9^\circ\text{C}$ , and temperature increases by  $\Delta T_{14} = 17.9^\circ\text{C}$ . Hence, temperature of

the input flow will be +20°C for the first cell part, +25.9°C for the second cell part, +34.8°C for the third cell part, +52.7°C for the fourth cell part.

Surface temperature of the first cell part will be  $T_{s1} = \Delta T_{21} + (T_{b1} + T_{b2})/2 = 29.9^\circ\text{C}$  ( $\Delta T_{21} = 6.9^\circ\text{C}$ ,  $\Delta T_{b1} = 20^\circ\text{C}$ ,  $\Delta T_{b2} = 25.9^\circ\text{C}$ ), of the second cell part  $T_{s2} = 40.9^\circ\text{C}$ , of the third cell part  $T_{s3} = 54.8^\circ\text{C}$  and of the fourth cell part  $T_{s4} = 76.7^\circ\text{C}$ .

Surface temperature for the fourth (upper) cell part increases by  $\approx 21^\circ\text{C}$ , and for the first (lowest) cell part decreases by  $\approx 25^\circ\text{C}$  compared to the case when the temperature of the entire surface is the same [7, 8].

Due to the friction at the channel walls air pressure along the channel length falls by  $\Delta p$  value, that can be calculated from the formula (15) and equals 12.8 Pa.

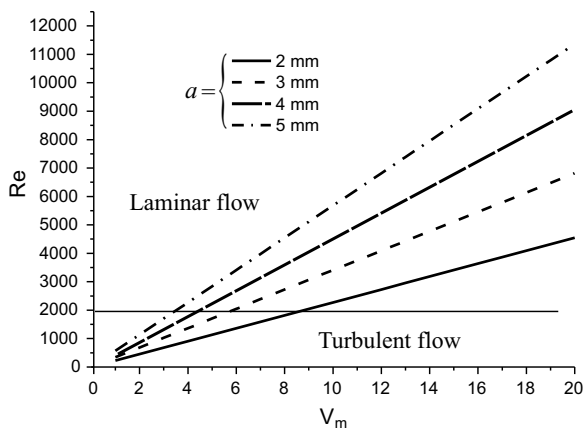


**Fig.4.**  $Re$  versus  $V_m$  for different gaps between battery cells

For the convenience of further calculations it is

necessary to know under what conditions the laminar air flow becomes turbulent. Dependence of the  $Re$  value on the air flow rate  $V_m$  and the gap between the cells  $a$  is shown at Fig. 4.

From Fig. 4 it is obvious that transition between laminar and turbulent flow occurs at  $V_m = 9\text{m/s}$  ( $a = 2\text{mm}$ ),  $V_m = 5.5\text{m/s}$  ( $a = 3\text{mm}$ ),  $V_m = 5\text{m/s}$  ( $a = 4\text{mm}$ ),  $V_m = 4\text{m/s}$  ( $a = 5\text{mm}$ ).

**The calculation for the turbulent flow.** We make calculations for air rate of  $V_m = 10\text{ m/s}$ , and the gap between the cells of  $a = 2\text{ mm}$ . In this case, the Reynolds number equals to  $Re = 2273$ , i.e. air-flow is turbulent. Nusselt number according to (14) equals to  $Nu = 10$ . Further calculations are similar to that one of the laminar flow. After  $k$ ,  $Nu$  and  $D_h$  calculation heat transfer coefficient value is obtained and equals to  $h_c = 66.7\text{ W/m}^2 \cdot \text{degree}$ . Air-mass flow for the channel equals to  $\dot{m} = 3.3\text{ g/s}$ . Then we calculated  $\Delta T_{21} = q_c / (h_c \cdot A) = 1.6^\circ\text{C}$  ( $q_c = 2\text{W}$ ,  $h_c = 66.7\text{W/m}^2 \cdot \text{degree}$ ,  $A = 2 \cdot 0.055\text{m} \cdot 0.15\text{m}$ ) for the first (lowest) cell part,  $\Delta T_{22} = 2.4^\circ\text{C}$  for the second,  $\Delta T_{23} = 3.2^\circ\text{C}$  for the third and for the fourth (upper)  $T_{24} = 4.8^\circ\text{C}$ . Knowing  $\Delta T_{21}$ ,  $\Delta T_{22}$ ,  $\Delta T_{23}$  and  $\Delta T_{24}$ , we calculated surface temperatures of the each cell.

Surface temperature of the first cell part  $T_{s1} = 22.2^\circ\text{C}$ , second  $T_{s2} = 23.7^\circ\text{C}$ , third  $T_{s3} = 25.7^\circ\text{C}$  and fourth cell part  $T_{s4} = 29^\circ\text{C}$ .

Similar calculations were done for  $V_m = 2 \dots 20\text{ m/s}$  and  $a = 3 \dots 5\text{ mm}$ . In the Table 2 and at Fig. 5 it is shown the calculations of the temperature of the fourth cell part  $T_{s4}$  versus air flow rate  $V_m$  gap between cells  $a = 2, 3, 4$  and  $5\text{ mm}$ .

**Table 2.**  $T_{s4}$  versus  $V_m$  and  $a$

$V_m, \text{ m/s}$	$a = 2\text{ mm}$	$a = 3\text{ mm}$	$a = 4\text{ mm}$	$a = 5\text{ mm}$
1	76.7	67.9	64.4	62.8
2	54.5	51.0	50.0	49.8
3	46.5	44.6	44.4	44.3
4	42.2	41.1	41.0	37.2
5	39.4	38.9	34.5	34.3
7	36.1	31.3	30.9	30.8
10	29.0	28.3	28.1	28.0
15	26.3	25.9	25.7	25.6
20	24.9	24.4	24.4	24.3

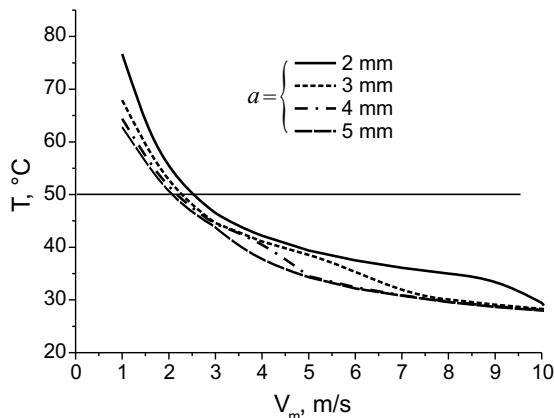


**Fig.5.**  $T_{s4}$  versus  $V_m$  and  $a$

From the calculated results it follows that the approach to the real conditions (the cell is divided into four parts), the temperature at the top of the cell exceeds the feasible conditions of the battery functioning ( $+50^\circ\text{C}$ ) and additional actions are needed to cool the battery cells. The cooling air supply from the top or side wall of the battery can be the simplest method.

#### 4. THE RESEARCH OF THE BATTERY WITH THE UPPER AIR SUPPLY

As most of the heat is released at the top of the battery cells, it is necessary to con-

sider the condition of the cell cooling for the upper air supply to the battery (Fig. 6).

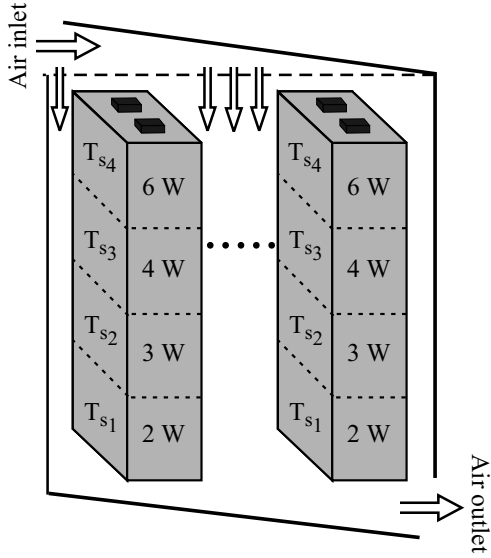


**Fig. 6.** Released power distribution in the battery cell with the upper air supply

In this case, the upper cell part is cooled by a cold stream, not yet warmed by passing the lower parts of the cells. Results of the comparison of calculations for the 2 mm gap between the cells when the air supplying from the bottom and top are given in Table 3 and Fig. 7 shows the dependence of the surface tem-

perature of the upper ( $T_{s4}$ ) and lower ( $T_{s1}$ ) cell parts on the cooling air flow rate.

Dependences are shown for the cases where air is supplied from the bottom ( $T_{s4}$ -bot), ( $T_{s1}$ -bot) and top ( $T_{s4}$ -top), ( $T_{s1}$ -top).

From Fig. 7 it is obvious that using the upper air supply temperature of the upper cell part it is possible to reduce the temperature of the surface of the cell upper part to below  $+50^\circ\text{C}$ . However, while the upper air supply temperature of the cell lower part increases to  $+63^\circ\text{C}$ . However, it is only observed at the air flow rate of  $V_m = 1 \text{ m/s}$ .

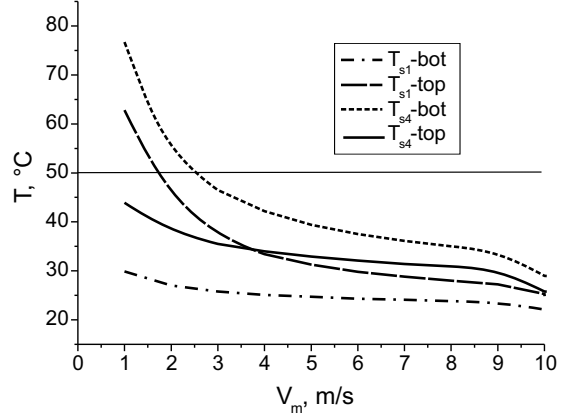


**Fig. 7.** Surface temperature of the first and fourth cell parts when cooling air is supplied from the bottom ( $T_{s4}$ -bot), ( $T_{s1}$ -bot) and top ( $T_{s4}$ -top), ( $T_{s1}$ -top) and  $V_m = 2 \text{ mm}$

**Table 3.** The results of calculations of the cell temperature for air supply from the top and bottom

$V_m, \text{ m/s}$	Supply from the top				Supply from the bottom			
	$T_{s1}, ^\circ\text{C}$	$T_{s2}, ^\circ\text{C}$	$T_{s3}, ^\circ\text{C}$	$T_{s4}, ^\circ\text{C}$	$T_{s1}, ^\circ\text{C}$	$T_{s2}, ^\circ\text{C}$	$T_{s3}, ^\circ\text{C}$	$T_{s4}, ^\circ\text{C}$
1	68.8	64.8	57.8	49.8	29.9	40.9	54.8	76.7
2	46.4	45.5	43.0	41.1	27.0	33.5	41.5	54.5
3	38.8	38.7	37.6	37.5	25.8	30.7	36.6	46.5
4	34.8	35.2	34.8	35.4	25.0	29.0	34.0	42.2
5	32.5	33.0	32.9	34.1	24.7	28.2	32.4	39.4
7	29.6	30.4	30.7	32.3	24.1	27.0	30.3	36.1
10	26.0	26.2	26.0	26.3	22.1	23.7	25.7	29.0
15	24.1	24.3	24.2	24.5	21.5	22.6	24.0	26.3
20	23.1	23.3	23.2	23.5	21.2	22.1	23.1	24.9

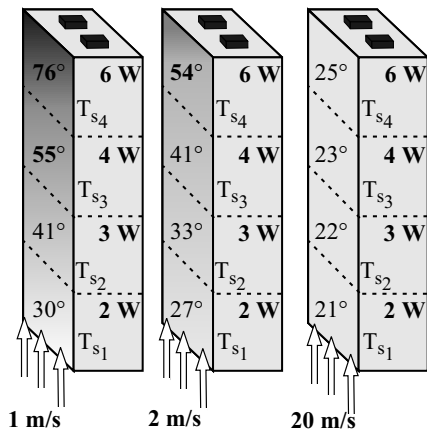


**Fig. 8.** Temperature distribution in separate cell parts for the air supply from the bottom ( $V_m = 1, 2, 20 \text{ m/s}$ , and  $a=2 \text{ mm}$ )

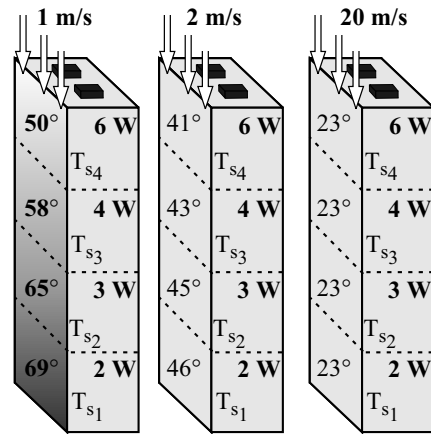


**Fig. 9.** Temperature distribution in separate cell parts for the air supply from the top ( $V_m = 1, 2, 20 \text{ m/s}$ , and  $a=2 \text{ mm}$ )

For greater clarity, at Fig.8 and Fig.9 it is shown the temperature distribution in the cell parts for the bottom (Fig.8) and the upper (Fig.9) the air supply. The temperatures in each cell part with air flow rates  $V_m = 1, 2$  and  $20$  m/s for the gap between the cells  $2$  mm are given. The temperature is rapidly increasing from the cell bottom to the top at a flow rate of  $V_m = 1$  m/s. At  $V_m = 2$  m/s temperature increasing is slower and it is almost insignificant at  $V_m = 20$  m/s.

### 5. INVESTIGATION OF BATTERY FUNCTIONING WHEN THE AIR IS SUPPLIED FROM THE LATERAL SURFACE

Let's consider battery cooling when the air is supplied from the lateral surface. All calculations will be done for air flow rate  $V_m = 1$  m/s and  $a=2$  mm.

We'll divide the cell wall into 4 parts in height (each part is  $0.055$ m high) and in width (each part is  $37.5$ mm) (Fig.10).

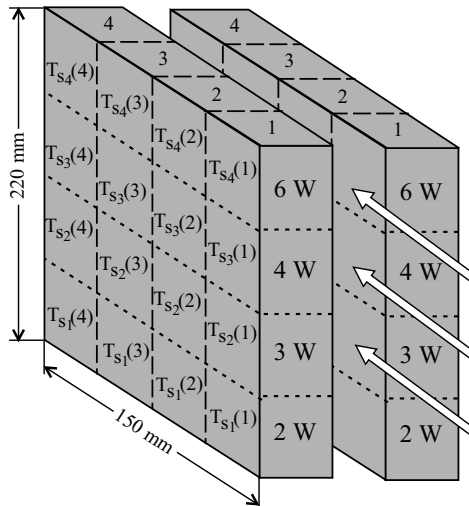


**Fig.10.** Battery cell presentation for the calculations of the cooling from lateral surface

As in the previous cases, let's say that from the 15 watts for the entire battery at the lowest (first) part of the cell  $2$  W is released, at the second in height -  $3$  W, at the third -  $4$  W and at the top -  $6$  W.

At first we'll consider detailed calculation of surface temperature only the fourth (top) part of the cell where the maximum power ( $6$  watts) is released and that the most difficult to cool. A detailed calculation of such system is given in [9]. Here we present only some results.

For the air flow rate of  $V_m = 1$  m/s, and the gap between the cells of  $a=2$  mm the Reynolds number equals to  $Re = 227$ , i.e. airflow is laminar. Nusselt number for air flow past surface of  $37.5$  mm equals to  $Nu = 4.8$ . After Nusselt number calculation heat transfer coefficient is obtained from formula (12) and equals to  $h_c = 31.8$  W/m<sup>2</sup>·degree.

Air flow of approximately  $\dot{m} \approx 0.11$  l/s will go through each separate cell part. In this case the

temperature of the cell part  $T_{s4}(1)$  (fig.10), will be  $T_{s4}(1)=34.8^\circ\text{C}$ , and other cell parts  $T_{s4}(2)=52^\circ\text{C}$ ,  $T_{s4}(3)=66^\circ\text{C}$ ,  $T_{s4}(4)=79^\circ\text{C}$ .

It is seen that when the air is supplied from the lateral surface the highest temperature is observed in the part of the cell (Fig. 10), which there is the output of the air flow. And this temperature is much higher than  $+50^\circ\text{C}$ .

The calculations for the other cell parts was done. The following results were obtained:

- for the third highest cell part (where  $4$ W is released)  $T_{s3}(1)=31.6^\circ\text{C}$ ,  $T_{s3}(2)=39.6^\circ\text{C}$ ,  $T_{s3}(3)=46.6^\circ\text{C}$ ,  $T_{s3}(4)=53.6^\circ\text{C}$ ;

- for the second highest cell part (where  $3$  W is released)  $T_{s2}(1)=28.7^\circ\text{C}$ ,  $T_{s2}(2)=34.7^\circ\text{C}$ ,  $T_{s2}(3)=40.7^\circ\text{C}$ ,  $T_{s2}(4)=46.7^\circ\text{C}$ ;

- for the first highest (lowest) cell part (where  $2$  W is released)  $T_{s1}(1)=26^\circ\text{C}$ ,  $T_{s1}(2)=30^\circ\text{C}$ ,  $T_{s1}(3)=34^\circ\text{C}$ ,  $T_{s1}(4)=38^\circ\text{C}$ .

The calculation results are given at Fig.11.

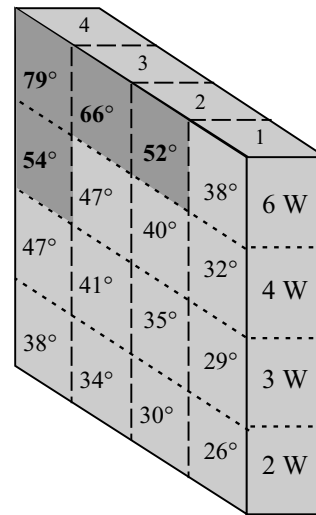


**Fig.11.** Calculation results of the cell part temperature for lateral air supply

We see that the temperature in the first, second and third cell parts are lower than in the top (fourth) part. This is due to the fact that in them the less power is released.

There is the question, how to reduce the temperature of the hot cell parts? Let's consider the variants:

1. To increase the air flow rate to  $2$  m/s, the gap between cells are the same  $a=2$  mm. In this case temperatures at the cell surface are  $T_{s4}(1)=32^\circ\text{C}$ ,  $T_{s4}(2)=36^\circ\text{C}$ ,  $T_{s4}(3)=40.6^\circ\text{C}$ ,  $T_{s4}(4)=45^\circ\text{C}$ . It is obvious, that increasing air flow rate to  $2$  m/s, it is possible to reduce significantly the temperature of the hottest cell part.

2. If the air flow rate  $V_m$  increases up to  $3$  m/s, than obtain  $T_{s4}(1)=30^\circ\text{C}$ ,  $T_{s4}(2)=34^\circ\text{C}$ ,  $T_{s4}(3)=38^\circ\text{C}$ ,  $T_{s4}(4)=42^\circ\text{C}$ . Therefore, as it was expected, with further air flow rate increasing the surface temperature will decrease.

3. To increase the gap between cells from  $a=2$  mm to  $a=3$  mm. Calculations will be done for  $V_m = 1$  m/s.

In this case the temperatures will be  $T_{s4}(1)=37.8^\circ\text{C}$ ,  $T_{s4}(2)=46.8^\circ\text{C}$ ,  $T_{s4}(3)=55.8^\circ\text{C}$ ,  $T_{s4}(4)=62.4^\circ\text{C}$ . I.e. gap increasing from  $a=2$  mm to  $a=3$  mm without rate changing ( $V_m=1$  m/s) doesn't results in surface temperature reducing below  $+50^\circ\text{C}$ .

In the future, we'll done calculations for different values of the gap between the cells and the various air flow rates. But from the above calculations the picture is rather clear.

**Analysis of the obtained results.** After the calculations of the battery cooling system with the bottom, top and lateral air supply it is necessary to compare

the results and make conclusions on the best method of cooling air flow supply into the battery.

All the conclusions are made for the specific design of the battery (see Fig.1), where the width of the battery  $b=150$  mm is less than of its height  $L=220$  mm. This is important for the case where the cooling air flow is supplied from the side and passes the smaller distance (150 mm) than for the cooling from bottom or top (220 mm).

The results of calculations of the cooling system obtained for different directions the cooling air flow are shown in Table 4.

**Table 4.** Calculation results of cooling system for bottom, top and lateral air supply

$a$ , mm	$V_m$ , m/s	Lateral supply, $^\circ\text{C}$					Bottom supply, $^\circ\text{C}$		Top supply, $^\circ\text{C}$	
		$T_{s4}(1)$	$T_{s4}(2)$	$T_{s4}(3)$	$T_{s4}(4)$	$T_s(\text{ave})$	$T_{s1}$	$T_{s4}$	$T_{s1}$	$T_{s4}$
2	1	37.3	51.8	65.5	79	58.4	29.9	76.7	68.8	49.8
2	2	32	36	40.6	45	38.4	27.0	54.5	46.4	41.1
2	3	30	34	38	42	37.5	25.8	46.5	38.8	37.5
3	1	37.8	46.8	55.8	62.8	50.8	29.9	67.9	55.8	49.8

When the lateral cooling air supply we introduced the quantity  $T_s(\text{ave})$  - the average temperature, which is equal to the value  $T_s(\text{ave})=(T_{s4}(1)+T_{s4}(2)+T_{s4}(3)+T_{s4}(4))/4$  (the temperature of all four parts of the surface of the top (fourth) of the cell are summed and divided by four), i.e. we take the mean value for the entire surface of the cell, and not only for the part of the surface where the air comes out. This may be the case when the heat from the output surface is rapidly spreading to the input surface.

The analysis of Table 4 shows that the highest temperature is observed in the upper part ( $T_{s4}$ ) of the cell surface during cooling from below ( $76.7^\circ\text{C}$ ), the surface temperature of the cell bottom ( $T_{s1}$ ) is somewhat lower for cooling from above ( $62.8^\circ\text{C}$ ) and surface of the upper cell part is best cooled  $T_s(\text{ave})$  ( $58.4^\circ\text{C}$ ) at lateral cooling. In this case, although the fourth part of the cell has a high temperature ( $79^\circ\text{C}$ ) at the air output, but the average temperature of the upper cell part of is not very high ( $58.4^\circ\text{C}$ ). It seems to happen due to the fact that the width of the battery (150 mm) shorter than its height (220 mm).

The general conclusion from all studies (changing speed and direction of the air supply to the battery, the gaps between the cells, etc.) is such that at low air flow rate of  $V_m=1$  m/s it is not possible to reduce the temperature of the cell surface below  $+50^\circ\text{C}$  and it is necessary to find other ways to solve this problem.

## 6. SEARCH OF THE EFFICIENT COOLING SYSTEM

Possible methods of effective cooling, i.e. creating conditions where the temperature of the hottest surface parts is less than  $+50^\circ\text{C}$ , may be obtained by increasing the  $h_c$  - heat transfer coefficient (12) or by increasing the Nusselt number (13, 14). In other words,

a possible way to create an efficient cooling system may come from studying the Nu number and the heat transfer coefficient  $h_c$  dependences on the in out air rate  $V_m$  for different values of the gap between the cells ( $a=2, 3, 4, 5$  mm). The results of calculations of the Nusselt number  $Nu$  and the heat transfer coefficient  $h_c$  are shown in Figs. 12 and 13, respectively.

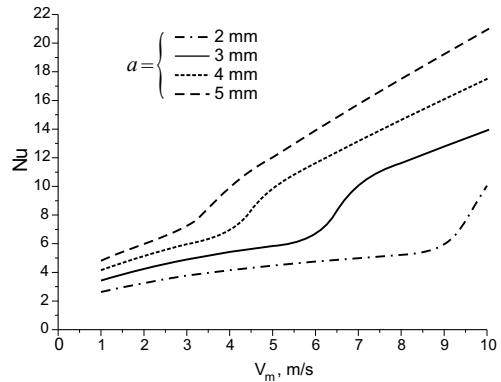


**Fig.12.** Nusselt number versus input air rate  $V_m$  ( $a=2, 3, 4, 5$  mm)

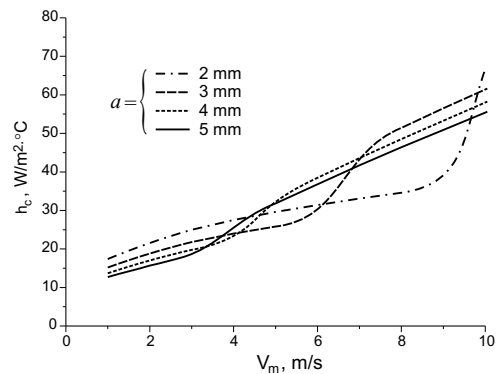


**Fig.13.** Heat transfer coefficient  $h_c$  versus input air rate  $V_m$  ( $2, 3, 4, 5$  mm)

It is obvious, that fracture is observed at the curves (Fig. 12), which corresponds to the transition from laminar to turbulent flow. At  $a=2$  mm fracture observed at  $V_m \approx 7-10$  m/s, at  $a=3$  mm - approximately at  $V_m \approx 5-7$  m/s, at  $a=4$  mm - approximately at  $V_m \approx 3.5-5$  m/s, at  $a=5$  mm - approximately at  $V_m \approx 3-4$  m/s.

It should be noted that the Nu number for the turbulent flow is significantly larger than for the laminar flow. In this case, the temperature of the upper cell part surface ( $T_{s4}$ ) for the turbulent flow is less than for the laminar, i.e. at the turbulent flow the cell surface is better cooled.

Therefore, we need to create such conditions when air flow will be turbulent even at low air flow rates. This can be done by turbulators, when there are various obstacles (rolling, individual petals, etc.) on the cell surfaces that transform laminar flow to turbulent flow. Such constructions of the turbulators are described in [10]. Research results with new turbulator designs will be considered in future articles.

From dependencies of the heat transfer coefficient  $h_c$  on  $V_m$  show at Fig. 13 it can be seen that at low rates  $V_m \leq 3$  m/s value is much smaller than at high flow rates.

We have previously noted (Fig. 5) that the temperature of the cell upper part is much higher than the maximum allowed temperature of  $+50^\circ\text{C}$  and this temperature can be reduced by increasing the heat transfer from the battery surface.

In 2010, American scientists have developed and published [11] a special coating that allows 3.5...4 times increasing the heat transfer from cooling surfaces. The development is based on nano- and microparticles of zinc oxide, which are deposited on surfaces using special devices. Layer of zinc oxide microparticles in the form of flowers are formed after such deposition. Another layer of particles of nanometer size is formed on the surface of these flowers. In the future, we will calculate and analyze the increasing the heat transfer from the surface with nanoparticle layer.

Preliminary results of the surface temperature at different air flow rates  $V_m$ , calculated for the gap between the cells of  $a=2$  mm are shown at Figs. 14 and 15.

The calculations were performed for the air supplied from the bottom (Fig. 3) for the first (lower) ( $T_{s1}$ -bot) cell part, and the fourth (upper) ( $T_{s4}$ -bot) cell part, for the air supplied from the top (Fig. 6) for the first (lower) ( $T_{s1}$ -top) cell part and the fourth (upper) ( $T_{s4}$ -top) cell part with and without nanoparticle layer.

Figs. 14 and 15 show that the cell surface temperature decreases when nanoparticle layer is applied. The temperature in most cases is less than  $+50^\circ\text{C}$ . However, even with nanoparticle layer, the temperature of the first (bottom) cell part at air supplied from the top is higher than  $50^\circ\text{C}$  when  $V_m=1$  m/s.

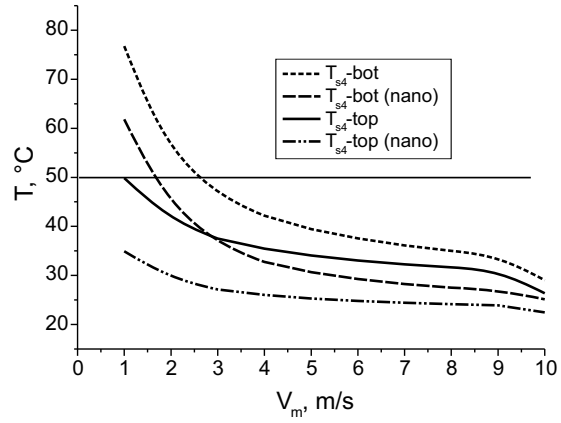


**Fig.14.** Temperature of the fourth (upper) cell part at air supplied from bottom and top without ( $T_{s4}$ -bot) and ( $T_{s4}$ -top) and with nanoparticle layer ( $T_{s4}$ -bot (nano)) and ( $T_{s4}$ -top (nano))

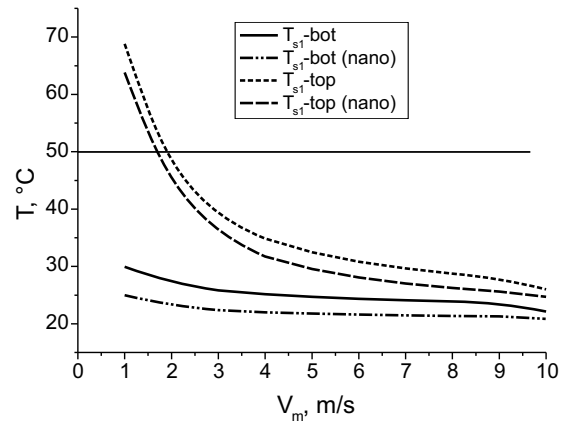


**Fig.15.** Temperature of the first (lower) cell part at air supplied from bottom and top without ( $T_{s1}$ -bot) and ( $T_{s1}$ -top) and with nanoparticle layer ( $T_{s1}$ -bot (nano)) and ( $T_{s1}$ -top (nano))

## 7. CONCLUSIONS

An analytical method for calculating the air flow battery cooling through a rectangular channel is considered. The results of calculations of cooling systems with non-uniform heat distribution in the battery cells for different air flow rates ( $V_m = 1 \dots 20$  m/s) and air supply directions - from bottom, top and side are given. The study is performed for gaps between the cells  $a = 2, 3, 4, 5$  mm. Efficiency of battery cooling batteries for different gaps between, air flow rates and directions were analyzed. It is shown that at low air flow rates (1 m/s) the cell temperature less than  $+50^\circ\text{C}$ , necessary to ensure normal battery operation, can not be obtained by any of the following methods. The air flow rates must be greater than 2 m/s to ensure the normal battery operation.

Preliminary results of calculation of the cooling system with special coating of the cell surfaces cells (nano-coating, which allows 3.5...4 times increasing the heat transfer from the battery surface, are given. It is shown that these technologies can significantly



reduce the cell surface temperature, but for the air rate of 1 m/s the hottest temperature of the battery may exceed the allowable temperature. Further researches must be done for the cooling system design to ensure the battery normal operation at low speeds of the cooling air.

## References

1. F. Krait, W. Black. *Heat Transfer Fundamentals*. Moscow: "Mir", 1983, 512 p. (in Russian).
2. X. Wong. *Basic formulas and data on heat transfer for engineers. Handbook*. Moscow: "Atomizdat", 1979, 216 p. (in Russian).
3. A.V. Teplov. *Hydraulics Fundamentals*. M.-L: "Energy", 1965, 447 p. (in Russian).
4. A. Pesaran. Battery Thermal Management in EVs and HEVs: Issues and Solutions. National Renewable Energy Laboratory. 1617 Cole Blvd. Golden, Colorado 80401 // *TAdvanced Automotive Battery Conference*. Las Vegas, Nevada, February 6-8, 2001.
5. Kim Gi-Heon, A. Pesaran. Battery Thermal Management System. Design Modeling // *EVS* 22. October 23-28, 2006, Yokohama Japan.
6. A. Pesaran. Battery Thermal Management in EVs and HEVs: Issues and Solutions // *First Annual Advanced Automotive Battery Conference*. Las Vegas, NV February 5-8, 2001.
7. R.P. Slabosritsky, M.A. Khazhmuradov, V.P. Lukyanova. Analysis and calculation of battery cooling system // *Radioelectronics and informatics*. 2011, N3, p. 3-8 (in Russian).
8. R.P. Slabosritsky, M.A. Khazhmuradov, V.P. Lukyanova. Studying of battery cooling system // *Radioelectronics and informatics*. 2012, N2, p. 5-8 (in Russian).
9. R.P. Slabosritsky, M.A. Khazhmuradov, V.P. Lukyanova. *The analytical calculation method for different colling system studying*. Preprint. KIPT, 2012, 22p. (in Russian).
10. E.K. Kalinin, G.A. Dreyzer, S.A. Yarkho. *Heat transfer in channels. 3rd edition, revised and enlarged, Mechanical Engineering*. 1990, 208 p. (in Russian).
11. T.J. Hendricks, S. Krishnan, et al. Enhancement of pool-boiling heat transfer using nanostructured surfaces on aluminum and cooper // *International Journal of Heat and Mass Transfer*. 2010, v. 53, iss. 15-16, p. 3357-3365.

## МЕТОД АНАЛИТИЧЕСКИХ РАСЧЕТОВ В ИССЛЕДОВАНИИ РАЗЛИЧНЫХ СИСТЕМ ОХЛАЖДЕНИЯ

*Р.П. Слабослицкий, М.А. Хажмуратов, В.П. Лукьянова, С.И. Прохорец*

Приведен аналитический метод расчета систем охлаждения аккумуляторных батарей потоком воздуха при неравномерном распределении тепла в ячейках батареи. Расчеты проведены для различных скоростей и направлений подачи воздуха. Показано, что обеспечить нормальную работу батареи можно только при скоростях потока воздуха больше 2 м/с.

## МЕТОД АНАЛІТИЧНИХ РОЗРАХУНКІВ В ДОСЛІДЖЕННІ РІЗНИХ СИСТЕМ ОХОЛОДЖЕННЯ

*Р.П. Слабослицкий, М.А. Хажмуратов, В.П. Лук'янова, С.І. Прохорець*

Приведено аналітичний метод розрахунку систем охолодження акумуляторних батарей потоком повітря при нерівномірному розподілі тепла в чарунках батареї. Розрахунки проведені для різних швидкостей і напрямів подачі повітря. Показано, що забезпечити нормальну роботу батареї можна тільки при швидкостях потоку повітря більше 2 м/с.